NASA Technical Memorandum 81747

Ion Beam Sputter Etching of Orthopedic Implant Alloy MP35N and Resulting Effects on Fatigue Properties

Edwin G. Wintucky and Mark Christopher
Lewis Research Center
Cleveland, Ohio
and
Eugene Bahnuik and Simon Wang
Case Western Reserve University
Cleveland, Ohio

Prepared for the
Fifteenth International Electric Propulsion Conference
cosponsored by the American Institute of Aeronautics and Astronautics,
the Japan Society for Aeronautical and Space Sciences,
and Deutsche Gesselschaft fur Luft- und Raumfahrt
Las Vegas, Nevada, April 21-23, 1981 (AIAA 81-0671)

NASA

ION BEAM SPUTTER ETCHING OF ORTHOPEDIC IMPLANT ALLOY MP35N AND RESULTING EFFECTS ON FATIGUE PROPERTIES

by
Edwin G. Wintucky and Mark Christopher
National Aeronautics and Space Administration
Lewis Research Center
Cleveland, Ohio

and
Eugene Bahnuik and Simon Wang
Case Western Reserve University
Cleveland, Ohio

ION BEAM SPUTTER ETCHING OF ORTHOPEDIC IMPLANT ALLOY MP35N AND RESULTING EFFECTS ON FATIGUE PROPERTIES

Edwin G. Wintucky* and Mark Christopher**
National Aeronautics and Space Administration
Lewis Research Center
Cleveland, Ohio

and

Eugene Bahnuik† and Simon Wang‡
Department of Mechanical and Aerospace Engineering
Case Western Reserve University
Cleveland, Ohio

ABSTRACT

The effects of two types of argon ion-sputter-etched surface structures on the tensile stress fatigue properties of orthopedic implant alloy MP35N were investigated. One surface structure was a natural texture resulting from direct bombardment by 1 keV argon ions. The other structure was a pattern of square holes milled into the surface by a 1 keV argon ion beam through a Ni screen mask. The etched surfaces were subjected to tensile stress only in fatigue tests designed to simulate the cyclic load conditions experienced by the stems of artificial hip joint implants. Both types of sputter-etched surface structures were found to reduce the fatigue strength below that of smooth surface MP35N.

INTRODUCTION

Over the past few years, an effort (ref. 1) at the Lewis Research Center has been directed toward identifying, evaluating and developing non-propulsive

---

*Physicist, Research and Advanced Concepts Section, Electrical Systems Branch, Space Propulsion and Power Division.

**Present address: Medical School, Ohio State University, Columbus, Ohio.

†Associate Professor

‡Graduate Student

applications (industrial and biomedical) of ion thruster technology. One promising biomedical application is the ion beam modification of surfaces of orthopedic implant materials for fixation to bone. Recent animal tests have shown that osseus tissue grows into the recesses formed on metal implant surfaces by ion beam sputter etching. Furthermore, the bonding and fixation properties of the implant are significantly enhanced. For example, a comparison between ion beam etched and smooth metal implants placed in dog tibia showed that forces up to 18 times greater were required to push out the ion beam etched implants (ref. 2).

The technique presently used for fixation of hip joint prostheses (examples shown in fig. 1) requires a grouting agent (polymethylmethacrylate) to secure the implant to the bone. These implants are subjected to high cyclic stress conditions with forces up to 1000 pounds (4.45×10^3 N) and as many as 10^6 stress cycles per year. Bone resorption and/or failure of the grouting agent often occurs, resulting in a loosening of the implant stem with a consequent increase in stress loading and ultimate fatigue failure of the stem. The X-ray photographs in figure 2 of an in vivo hip joint implant show an actual stem fracture resulting from fatigue failure. To avoid this problem, it is desirable to develop a stable non-grouted prosthesis where the bone attaches directly to the implant. Because of the superior attachment resulting from bone ingrowth to structured surfaces, ion beam technology can possibly make a significant contribution to this development.

In regions of tensile stress, surface defects such as scratches, notches, voids and inclusions can cause locally high stress concentrations. These defects are potential sites for the initiation of fatigue cracks, the propagation of which is often the cause of premature fatigue failure.

A question of importance is what effect does ion beam etched surface structure have on the fatigue strength of orthopedic alloys. Preliminary tests on a few specimens of ion beam textured orthopedic alloys, for example, Ti-6%A1-4%V, suggested some degradation of fatigue strength (ref. 3). To more fully answer the question, a more thorough and systematic characterization of the fatigue properties of an orthopedic alloy was undertaken. The material chosen for the study was MP35N (Latrobe Steel Co., Latrobe, PA), a work-strengthened, high tensile strength, ductile, corrosion-resistant, multiphase alloy with a typical composition of 35 percent Co, 35 percent Ni, 20 percent Cr and 10 percent Mo (ref. 4). Because of its properties,

MP35N is now being increasingly used for orthopedic surgical implants (refs. 5 to 8).

The fatigue behavior of MP35N having three types of surface finishes was evaluated under bending stress conditions. The surface finishes were (1) a smooth, untextured finish, (2) a natural texture generated by direct ion beam sputtering and (3) a regular pattern of square holes produced by ion beam etching through a Ni screen mask in contact with the surface. The bending stress fatigue tests were designed to simulate the cyclic load conditions experienced by the stems of hip joint prostheses, which is where fatigue failure usually occurs (fig. 2). The fatigue specimens were placed in contact with a physiological saline solution to simulate the corrosive electrolytic fluids which naturally bathe the implant in a human body environment.

This paper presents fatigue test results demonstrating the effects of the two different ion beam sputter-etched surface structures on the fatigue behavior of MP35N over a cycle range of 10^4 to 1.7×10^7 cycles. Possible thermal effects resulting from ion bombardment heating are also considered.

APPARATUS AND PROCEDURE

Fabrication of Fatigue Test Specimens

The high tensile strength and ductility of MP35N are achieved through a combination of cold work strengthening and aging (refs. 3 and 4). The MP35N used in this study was cold rolled into a 0.387-inch-thick (9.83-mm) plate, with a 60 to 63 percent reduction in thickness, followed by four hours of aging at a temperature of approximately 560° C (AMAX Specialty Metals, Cleveland, Ohio). The resulting mechanical properties of the cold rolled and aged MP35N (ref. 9), shown in table I, complied with the ASTM specifications for surgical implant applications. The surface hardness numbers measured to be 48 Rc (Rockwell-c). Elemental analysis of the MP35N showed the chemical composition to be within the requirements specified for orthopedic implant applications (refs. 5 and 9).

The fatigue test specimens (fig. 3) were ground to the geometry and dimensions shown in figure 4, the shaded area being the test section. The

specimen geometry was that typically used in bending fatigue tests. The specimen thickness of 0.375 inches (9.53 mm) was similar to the stem thickness of hip joint implants. The surfaces of the test sections were polished to within a 15 microinch (0.38 μm) RMS finish. The test surfaces of the specimens with the smooth finish were further polished with a 600 grade emery cloth parallel to the longitudinal direction.

Sputter Etching of Surfaces

Both types of sputter-etched surface structures were produced by 1 keV ions from 30-cm diameter argon ion sources, whose construction and operating principles are detailed in reference 10, in a 1.5-m diameter by 4.5-m long vacuum facility.

Natural Texture Generated by Direct Ion Bombardment. - Under direct ion bombardment, MP35N develops a natural surface texture. This surface texture is more readily produced at ion current densities higher than that generally available in the ion beam from conventionally operated ion sources. The desired ion current densities were more conveniently and simply obtained by operating the ion source in a DC triode sputtering configuration. The ion extraction grids were removed from the source and replaced by an electrically isolated plate with an orifice of the same geometry as the test section of the fatigue specimen (fig. 5). Argon ions were extracted from the source and caused to bombard the top surface of the test section by biasing the target specimen 1000 V negative relative to the discharge chamber plasma potential. The small square hole on the side of the test section (fig. 5) was to enable the sputter etching of a 1-cm square MP35N control sample simultaneously with the fatigue specimen.

Figure 6 is a photograph of the ion source mounted in the vacuum facility. Figure 7 shows schematically the sputter-etching arrangement of the ion source and the target specimen. The etch conditions used to sputter the natural texture are summarized in table II. The energy of the bombarding ions was 1 keV at current densities of around 6 mA/cm^2. Etch times were typically 2 to 2.5 hours. A Chromel-Alumel thermocouple mounted on the underside

of the specimen indicated temperatures in the range of 450° to 500° C during ion bombardment. Argon gas was introduced into the discharge chamber through the main cathode at a typical flow rate of about 30 standard cc/min (SCCM). The corresponding indicated vacuum facility pressure in the vicinity of the ion source was around 3×10^{-5} torr.

Figure 8 is a Scanning Electron Microscope (SEM) photograph of a smooth finish, untextured MP35N surface (300×). The striations on the surface are abrasion marks resulting from polishing the surface and are parallel to the rolling direction. The ion beam natural texture surfaces were medium to dark grey in color. Figure 9 shows an example of the natural textured surface of a fatigue specimen test section. Also shown is a simultaneously textured 1-cm square control sample. SEM photographs of the natural texture at magnifications of 300×, 3000× and 10 000× are shown in figure 10. As figure 10 shows, the surface texture on MP35N, produced under the ion bombardment conditions described above, consisted of a coarse, lumpy structure whose dimensions were on the order of tens of microns, on which was superimposed a finer ridge-like structure whose dimensions were on the order of tenths of microns.

Square Hole Pattern. - The 30-cm diameter argon ion source used for ion beam etching the square hole pattern is shown in figure 11. The source was operated in a conventional manner with the ion extraction grids masked to an active diameter of 10 cm. Figure 12 shows schematically the ion etching arrangement of ion source and fatigue specimen. The etch conditions are summarized in table II. The fatigue specimens were positioned 10 cm downstream from the ion extraction grids where the ion current density was maintained in the range of 1.5 to 2.0 mA/cm^2. Ion energies were 1 keV. Etch times were typically 16 to 17 hours, which was also approximately the length of time required to sputter etch away the 125-μm-thick electroformed Ni mesh (Buckbee-Mears Co., St. Paul, MN) used as a sputter mask. Argon gas flow was 100 to 110 SCCM through the main cathode. The corresponding vacuum facility pressure in the vicinity of the ion source was around 10^{-4} torr.

A representative square hole pattern etched into an MP35N surface, photographed with an optical microscope at a magnification of 40×, is

shown in figure 13. The holes in the Ni mesh were 150 μm × 150 μm on 280 μm centers. The etched holes ranged from 150 μm to 200 μm at the top and 120 μm to 140 μm at the bottom. Hole depths ranged from 70 to 100 μm with most around 90 μm. Figure 14 is a photograph taken at the edge of the sample with an optical microscope at a magnification of 100× and shows the tapered geometry of the etched holes. The holes shown in figure 14 appear deeper than the completely enclosed holes because there was less material sputtered from the walls for redeposition at the bottom of the holes. A typical etched hole structure is shown in the SEM photographs in figure 15 at magnifications of 100× and 300×.

The sharpness of the etched hole structure depended on both the amount of etching after the Ni mesh was sputtered away and the proximity of the Ni mesh to the MP35N surface during etching. The difference in thermal expansions of the Ni mesh and the MP35N made it difficult to maintain close contact between the two. A uniformly sharp etch pattern over the entire test section was not always obtained. The sharpest structure was obtained by mounting the Ni mesh in a stainless steel frame (shown in fig. 3) and spot welding the frame to the fatigue specimen at the edges of test section. The Ni mesh was then also attached to stainless steel strips which conformed to the shape of the sides of the test section.

Fatigue Tests

During walking, climbing, running, jumping and other similar body movements, the moment of force applied to the stem of a hip joint implant typically varies from zero to some positive value, depending on body weight and length of moment arm. Such loading of an implant stem can be approximated by pure bending (ref. 11). By definition, only normal stresses are present on the cross-section in pure bending, varying from tension on one side to compression on the other. A representative cross-section with the distortion resulting from bending is shown in figure 16. Passing through the centroid of the cross section is a line called the neutral axis, along which the stress and strain are zero. Pure bending is achieved by loading the specimen with equal and opposite force couples at the ends, which is also

called the four-point bending mode. Figure 17 shows a free-body diagram of the distribution of applied load, P, in the four-point bending mode, together with the corresponding variation of bending moment, M, along the specimen. The section between points X and Y corresponds to the test section of the fatigue specimen. As figure 17 indicates, the bending moment is constant across this section and equal to PL/2 where L is the moment arm. Figure 18 shows the four-point bending fixture holding a fatigue specimen.

Within the elastic range, the stress varies directly with distance from the neutral axis (fig. 16). The maximum stress occurs at the surfaces, where elongation or compression are the greatest, and is simply related to the bending moment and applied load according to the equation

$$S = \frac{Mc}{I} = \frac{PLc}{2I}$$

c is the distance of the surface from the neutral axis and is equal to half the specimen thickness. I is the moment of inertia of the cross-section about the neutral axis. This equation was used to calculate stress from the applied load in the fatigue tests. For rectangular cross-sections as in the test sections of the fatigue specimens, $I = Ac^2/3$ where A is the cross-section area. For a specimen of uniform thickness, the maximum stress obviously occurs where A is the smallest, which would be the narrowest part of the test section.

The fatigue testing machine was a Sonntag SF-1-V operated at 30 Hz. Because fatigue cracks usually initiate on the tensile stress side of the implant stem, the treated surfaces of the fatigue specimens were subjected to tensile stress only. This was accomplished by preloading the specimens to eliminate reverse bending. A combination of steady and alternating stresses were thus applied to the specimens. The minimum stress, S_{min}, was zero. The mean stress, $S_m = \frac{1}{2}(S_{max} + S_{min})$ was equal to the stress amplitude, $S_a = \frac{1}{2}(S_{max} - S_{min})$. The stress ratio, $R = S_{min}/S_{max}$, was zero. Figure 19 shows the sinusoidal variation of applied stress for both $R = 0$ and $R = -1$, the latter being the case for pure alternating stress, i.e., complete reverse bending. The stress terminology is as defined in ASTM E 206-72.

Twenty specimens of each type of surface finish were fatigue tested. Load settings were were chosen to correspond to estimated fatigue lives ranging from 10^4 up to 1.7×10^7 cycles. Several specimens were cycled at each load setting or for a maximum of 1.7×10^7 cycles, which is nearly equivalent to the number of cycles the stem of an artificial hip joint would undergo over a 20-year period. Maximum stress levels ranged from near 10 ksi (69 MPa) to about 100 ksi (690 MPa).

The fatigue tests were conducted at room temperature (20^o C) with the test sections immersed in an artificial physiological solution formulated to simulate the corrosive environment of the human body (ref. 12). The physiological solution was saline with a pH of 7 and a composition of 8.74 g/ℓ NaCl, 0.35 g/ℓ $NaHCO_3$, 0.06 g/ℓ Na_2HPO_4 and 0.06 g/ℓ NaH_2PO_4. The physiological solution was successfully contained in a rubber tube surrounding the test section, shown in figure 20. The rubber tube was sealed at both ends by a combination of epoxy and silicon rubber cements. Five ml of solution were injected into the rubber tube and the air removed. The fatigue specimens were also presoaked for one week in the physiological solution prior to fatigue testing.

Pure Tensile Tests

Limited pure tensile testing of the fatigue specimens was performed for the purpose of observing what large scale effects ion beam processing might have on the ultimate tensile strength of MP35N. The ultimate tensile strength was measured by conventional procedure with an Instron tensile testing machine on one fatigue specimen for each type of surface finish.

RESULTS AND DISCUSSION

The primary results of the tensile stress fatigue tests are shown in the S-N diagram in figure 21, which is a log-log plot of stress amplitude (maximum stress) versus number of cycles for the actual test data for each of the three surface finishes. The straight lines are the estimated stress amplitudes fitted to the test data according to the least squares estimation procedure of linear regression analysis. The equations for the linear

regression lines are given in table III. As figure 21 indicates, both types of ion beam sputter-etched surface structures resulted in a significant reduction in fatigue strength at high cycle life ($> 10^5$ cycles), with the square hole pattern showing the largest reduction. The highest number of cycles at which fatigue failure was actually observed for any of the three surface finishes was around 5×10^6 cycles, which is estimated to be about the number of load cycles a hip joint implant would undergo over a 5-year period. At 5×10^6 cycles, the estimated fatigue strengths (table III) of the ion beam textured surface, 28.1 ksi (194 MPa) and the pattern etched surface, 23.0 ksi (159 MPa), were approximately 48.3 percent and 39.6 percent, respectively, of the estimated fatigue strength of the smooth surface, 58.2 ksi (401 MPa).

A typical example of an MP35N test specimen after fatigue failure is shown in figure 22. Figure 23 shows typical fractures at a magnification of 100× of MP35N fatigue specimens with the natural ion beam etched texture and the square hole pattern surface structure. As figure 23 illustrates, the fatigue cracks generally followed the edges of the square holes, which were probable sites of locally high stress concentration.

The S-N diagram in figure 21 represents the fatigue test results for a combination of applied steady and alternating stresses in which the stress, amplitude, S_a, equalled the mean stress, S_m, and the stress ratio R = 0. In this way, the test surfaces of the fatigue specimens were subjected to tensile stress only and the fatigue tests thereby simulated the actual cyclic loading conditions experienced by the stem of a hip joint implant. The fatigue test results for R = 0 are, therefore, of direct interest to the implant designer.

Fatigue data is commonly presented on S-N diagrams for the case of pure alternating stress, where $S_m = 0$, $S_a = S_{max}$ and R = -1 (fig. 19(b)). The R = -1 representation usually enables a more convenient comparison of fatigue test data with values predicted by relationships based on tensile data, as in the method of universal slopes, for example (ref. 13). The fatigue behavior of cold worked and aged MP35N documented by this investigation should add to the growing body of knowledge of the mechanical properties of that alloy. Therefore, for general reference purposes, the S-N diagram for R = -1, based on the test data for R = 0, is presented here.

The stress amplitude for pure alternating stress (R = -1) can be estimated from the stress amplitude for R = 0 by means of Goodman's mean stress law, which postulates a linear variation of stress amplitude with mean stress (ref. 11). For a given cycle life, the stress amplitudes are related by

$$\frac{1}{S_a(R=-1)} = \frac{1}{S_a(R=0)} - \frac{1}{S_u}$$

where S_u is the ultimate tensile strength. The Goodman mean stress diagram for MP35N with the smooth surface finish is shown in figure 24 and illustrates the relationship between the stress amplitudes for R = 0 and R = -1. Figure 25 is the S-N diagram for R = -1 representing the fatigue behavior of the three types of surface finishes.

Heating of the target occurs naturally during ion bombardment. The temperatures of the square hole pattern etched specimens during ion bombardment, although not measured, were estimated from other experiments to be less than 400° C. Temperatures in the range of 450° to 500° C were measured on the underside of the fatigue specimens during ion etching of the natural texture (2 to 2.5 hr). The temperatures of the top surfaces and bulk of the test sections were somewhat higher, possibly as high as 750° C. This temperature is well below the annealing temperature of MP35N (~ 1050° C) but well above precipitation strengthening or aging temperature (~ 560° C for 4 hr). The possibility that thermal effects, as well as irregular surface structure, could have influenced the fatigue behavior is, therefore, an important consideration.

In an attempt to determine possible thermal effects, two MP35N specimens were heated for two hours in vacuum, one at 500° C and the other at 660° C, and then fatigue tested. The fatigue test results are shown in figure 21 as points A (500° C) and B (660° C). Specimen A (500° C) indicated no reduction in fatigue strength, 54.23 ksi (374 MPa) at 7.954×10^6 cycles. The result for specimen A supports the expectation that heating MP35N to temperatures below the aging temperature does not change its mechanical properties. However, a significant reduction in fatigue strength, 44.21 ksi (305 MPa) at 6.05×10^6 cycles, was

indicated by sample B (660° C). Additional thermal aging of MP35N at temperatures above that necessary for precipitation strengthening (560° C) would result in a decrease in ductility (ref. 4). The increase in brittleness could produce a corresponding reduction in fatigue strength, as evidenced by the fatigue test result for specimen B (660° C for 2 hr). The implication is that thermal effects could have made a significant contribution to the reduction in fatigue strength of the naturally textured MP35N, which experienced temperatures possibly as high as 750° C during the 2-hour ion-sputter-etch process. On the other hand, the square hole pattern-etched MP35N temperatures during ion bombardment were estimated to be less than 400° C, well below the aging temperature. In that case, thermal effects on mechanical properties would be expected to be negligible. Consequently, the reduction in fatigue strength exhibited by the square hole pattern etched MP35N can be attributed to the irregular surface structure.

Other tests did not indicate any temperature effects. Both types of ion beam etched surface structures showed an average surface hardness of 47 Rc, only slightly less than the hardness of the unetched surface which was 48 to 49 Rc. Metallographic examination of cross-sections of sputter-etched and unetched MP35N samples did not reveal any notable differences in grain structure. The ultimate yield strengths were measured on one fatigue specimen of each type of surface finish using the pure tensile testing procedure described in the apparatus and procedure section. The results, shown in table IV, were all approximately the same as that of the original material.

CONCLUDING REMARKS

Both types of ion beam sputter-etched surface structure were found to reduce the fatigue strength below that of MP35N with a smooth surface finish over the range from 5×10^4 to 1.7×10^7 cycles. For example, at 5×10^6 cycles, the estimated fatigue strength of the square hole structure was reduced by approximately 60 percent, whereas the estimated fatigue strength of the sputter-etched natural texture was reduced by approximately 50 percent. Thermal effects resulting from ion bombardment heating, in

addition to surface structure, may have possibly also contributed to the observed reduced fatigue strength of the naturally textured MP35N.

The results of this fatigue study are important for implant design. Because of the potentially large gains in implant fixation offered by direct bone ingrowth, ways to lessen or offset the reduction in fatigue strength for sputter-etched surface structures merit consideration. Optimum bone ingrowth occurs in recesses on the order of 150 to 200 μm. For this reason, the square hole geometry is potentially more useful than the sputter-etched natural texture. With its abundance of sharp edges and corners, the square hole geometry as tested here probably presents more sites of large stress concentration than any other geometry. A possible way to reduce the stress concentration for this geometry, and thereby improve fatigue strength, would be rounding of the hole edges by ion beam polishing of sputter etched surface. Another possibility is a hole geometry which has fewer sharp corners, such as round holes. A hexagonal, rather than a rectangular, hole array might also be considered.

It is possible that direct bone ingrowth could result in less tensile stress of the implant than occurs with the present technique using a grouting agent to attach the implant to the bone. Further studies would be required to assess this possibility. A way of preventing reduction in fatigue strength would be to sputter etch holes only in the low tensile stress areas of the implant, such as along the neutral bending axis and on the compressive side. In any case, it would be important to avoid any adverse thermal effects by maintaining the MP35N temperature below the aging temperature during ion beam processing.

REFERENCES

1. Banks, B. A., "Ion Beam Applications Research - Lewis Research Center, 1981," AIAA Paper 81-0669, April 1981.
2. Gibbons, D. F., "The Evaluation of Surface Texture by Ion Beam Sputtering on the Mechanical Fixation and Biological Compatibility of Orthopedic Alloys in Bone," NASA Grant NSG-3151, Case Western Reserve University, 1979.
3. Weigandt, A. J., "Mechanical Properties of Ion Beam Textured Surgical Implant Alloys," NASA TM-73742, 1977.

4. "MP35N Alloy," Product Information Bulletin, Latrobe Steel Company, Latrobe, PA., 1977.
5. "Standard Specification for Wrought Cobalt-Nickel-Chromium-Molybdenum Alloy for Surgical Implant Applications," Annual Book of Standards, American Society for Testing and Materials, ANSI/ASTM-F562-78, Pt. 46, 1980, pp. 1012-1014.
6. Gachter, A. and Galante, J., "MP35N, A Corrosion Resistant High-Strength Alloy for Orthopaedic or Surgical Implants: Two Year Bioassay Results," Journal of Biomedical Materials Research, Vol. 10, 1976, pp. 829-831.
7. Escalas, F., Galante, J., Rostoker, W., and Coogan, P. S., "MP35N, A Corrosion Resistant High-Strength Alloy for Orthopaedic Surgical Implants: Bioassay Results," Journal of Biomedical Materials Research, Vol. 9, 1975, pp. 303-313.
8. Baumann, R., and Semlitsch, M., "Biological and Mechanical Behaviour of Newly Developed Implant Materials in Animal Studies," Sulzer Technical Review, Vol. 56, 1974, pp. 118-125.
9. "Material Certification Report, AMAX No. 2789," AMAX Specialty Metals Corporation, Cleveland, OH, August 1979.
10. Sovey, J. S., "30-Cm Diameter Argon Ion Source," AIAA Paper 76-1017, November 1976.
11. Richards, C. W., Engineering Materials Science, Wadsworth Publishing Company, San Francisco, 1961.
12. Cigada, A., Mazza, B., Pedeferri, P., and Sinigaglia, D., "Influence of Cold Plastic-Deformation on Critical Pitting Potential of AISI 316L and 304L Steels in an Artificial Physiological Solution Simulating the Aggressiveness of the Human Body," Journal of Biomedical Materials Research, Vol. 11, 1977, pp. 503-512.
13. Manson, S. S., "Fatigue: A Complex Subject - Some Simple Approximations," Experimental Mechanics, Vol. 5, July 1965, pp. 193-226.

TABLE I. - MECHANICAL PROPERTIES (MINIMUM VALUES, GAGE LENGTH 1 INCH (25.4 mm)) COLD ROLLED AND AGED MP35N USED IN FATIGUE TESTS (REF. 9). TENSILE TESTS CONDUCTED IN COMPLIANCE WITH ASTM E-8

	Ultimate tensile strength, ksi (MPa)	0.2% Yield strength, ksi (MPa)	Area reduction (%)	Elongation (%)
Longitudinal *	247 (1700) 245 (1690)	232 (1600) 240 (1650)	54.0	10.0 10.0
Transverse	249 (1720) 245 (1690)	235 (1620) 241 (1660)	50.0	9.0 8.0

*In the direction of rolling.

TABLE II. - SUMMARY OF ION BEAM SPUTTER ETCH CONDITIONS USED TO PRODUCE BOTH TYPES OF SURFACE STRUCTURE

	Natural texture	Square hole pattern
Ion energy (eV)	1000	1000
Ion current density (mA/cm^2)	6	1.5 to 2
Etch time (hr)	2 to 2.5	16 to 17
Sample temperature (deg C)	450 to 500*	Not measured

*Measured on underside of target specimen with Chromel-Alumel thermocouple.

TABLE III. - LINEAR REGRESSION EQUATIONS, $\log S = a \log N + b$, AND ESTIMATED FATIGUE STRENGTHS AT 5×10^6 CYCLES FOR THE THREE TYPES OF SURFACE FINISHES

Surface finish	a	b	Correlation coefficient	Estimated fatigue strength at $N=5\times10^6$ cycles, ksi (MPa)
Smooth	-0.0911	2.3743	-0.904	58.2 (401)
Natural ion etched texture	-0.2427	3.0746	-0.991	28.1 (194)
Ion beam etched square hole pattern	-0.2527	3.0553	-0.988	23.0 (159)

TABLE IV. - ULTIMATE TENSILE STRENGTHS OF MP35N FATIGUE SPECIMENS WITH THE THREE TYPES OF SURFACE FINISHES

Surface finish	Ultimate tensile strength, ksi (MPa)
Smooth	246 (1695)
Natural ion beam texture	250 (1725)
Etched square hole pattern	250.5 (1727)

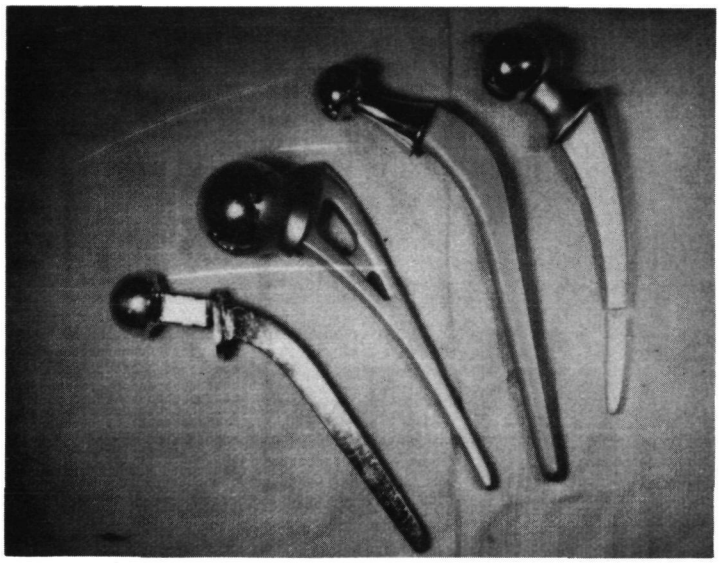

Figure 1. - Examples of artificial hip joint implants.

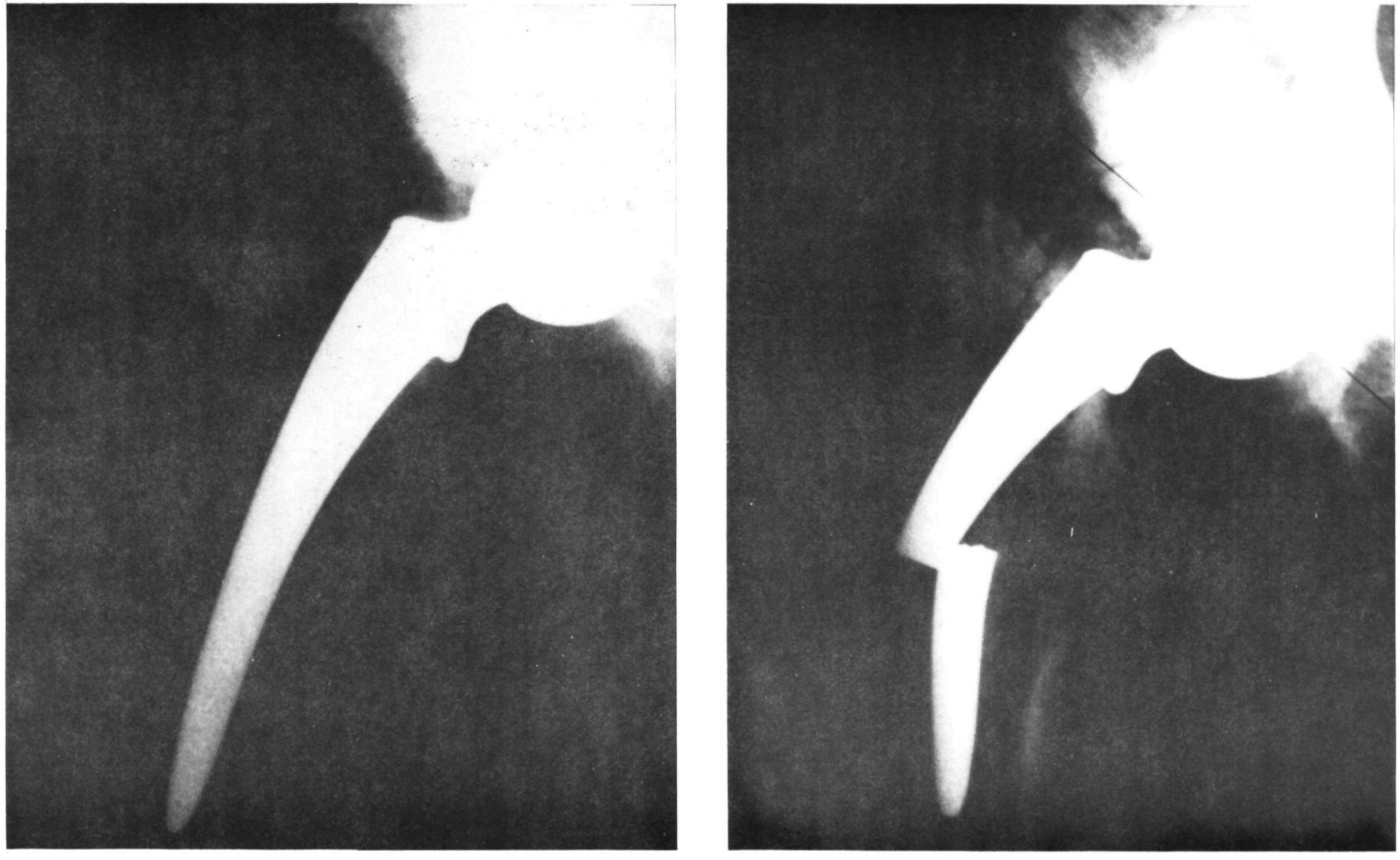

(a) BEFORE. (b) AFTER.

Figure 2. - X-ray photographs of an in vivo hip joint implant (a) before and (b) after fatigue failure.

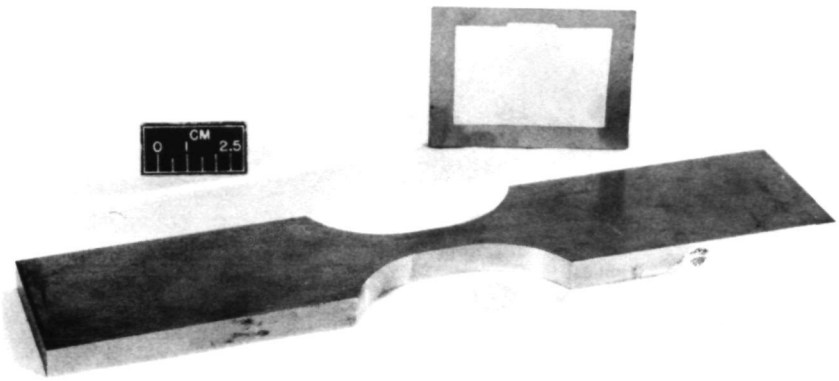

C-80-1888

Figure 3. - MP35N fatigue test specimen. Also shown is Ni mesh mask for ion beam etching square hole pattern.

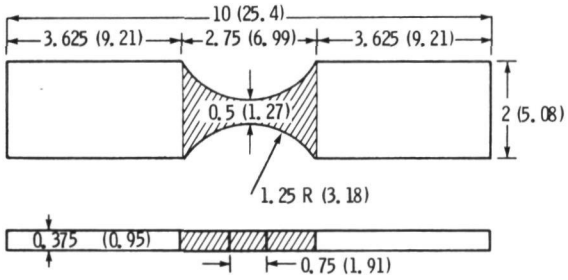

Figure 4. - Geometry and dimensions of fatigue test specimen. Test section is shaded area. Dimensions are in inches (cm).

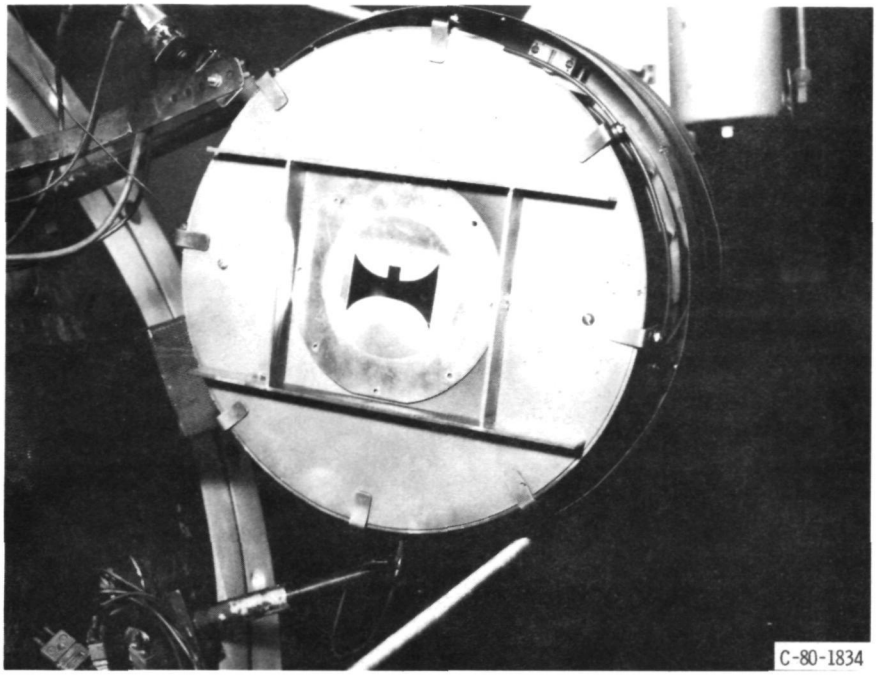

Figure 5. - Orifice through which ions were extracted from discharge chamber for bombardment of fatigue specimen test section and 1 cm square control sample.

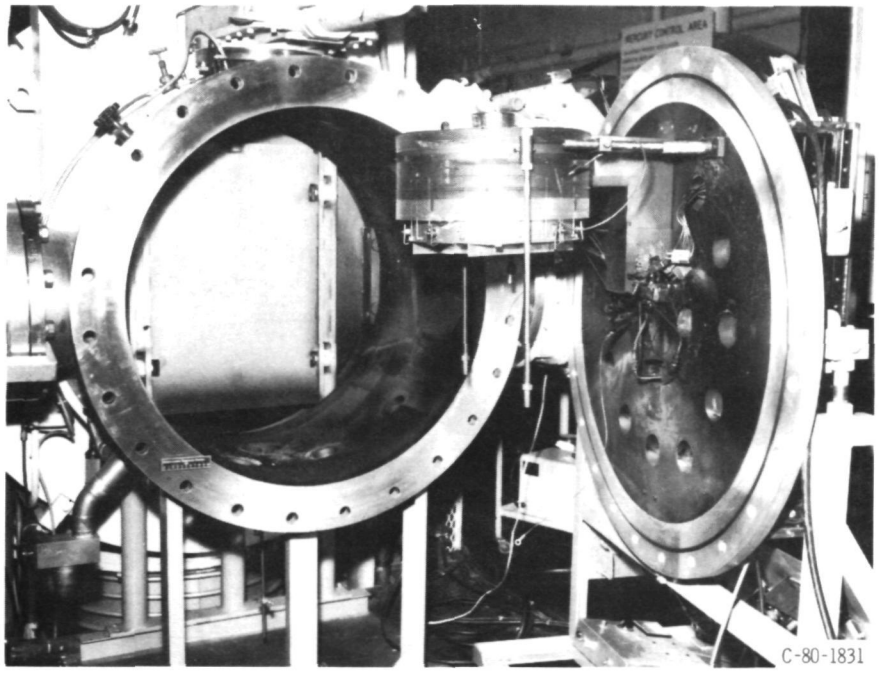

Figure 6. - Ion source used to produce natural texture shown mounted in test facility.

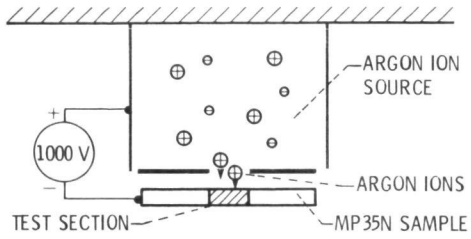

Figure 7. - Schematic arrangement of ion source and target specimen for sputtering of natural ion beam-etched surface structure. Power supply arrangement given in reference 1.

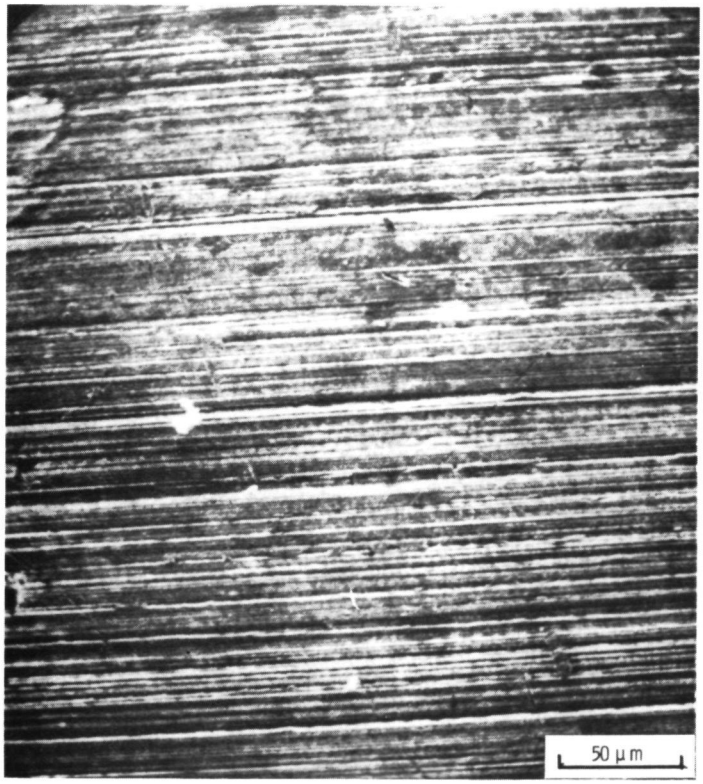

Figure 8. - SEM photograph (300X) of smooth finish, untextured MP35N surface. Striations are abrasion marks from polishing and are parallel to direction of rolling and longitudinal axis of fatigue specimen.

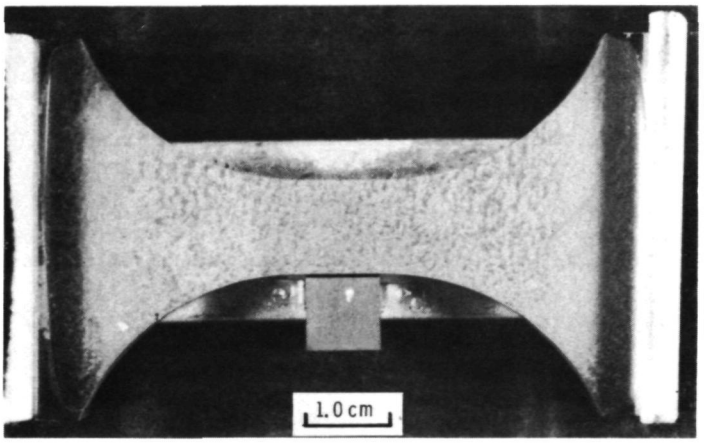

Figure 9. - Example of naturally textured surface of fatigue specimen test section.

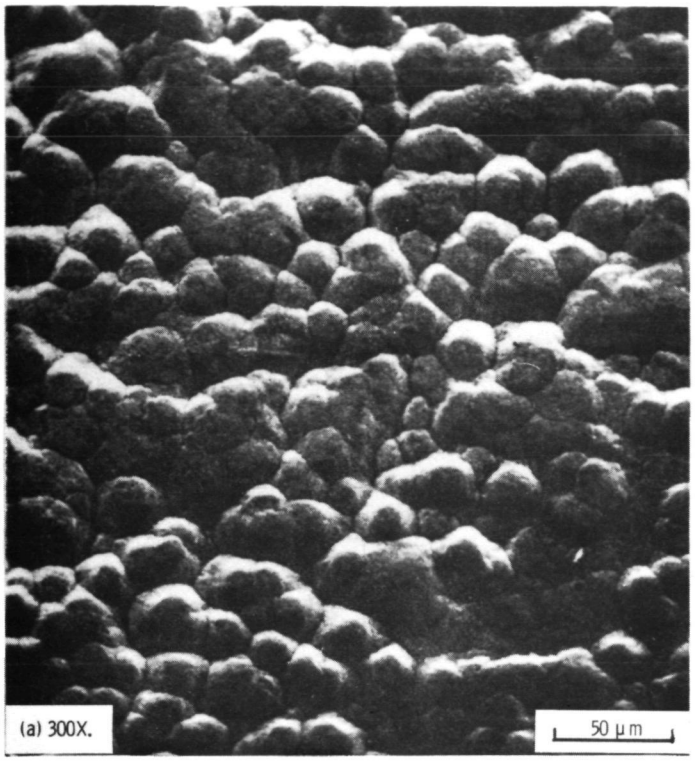

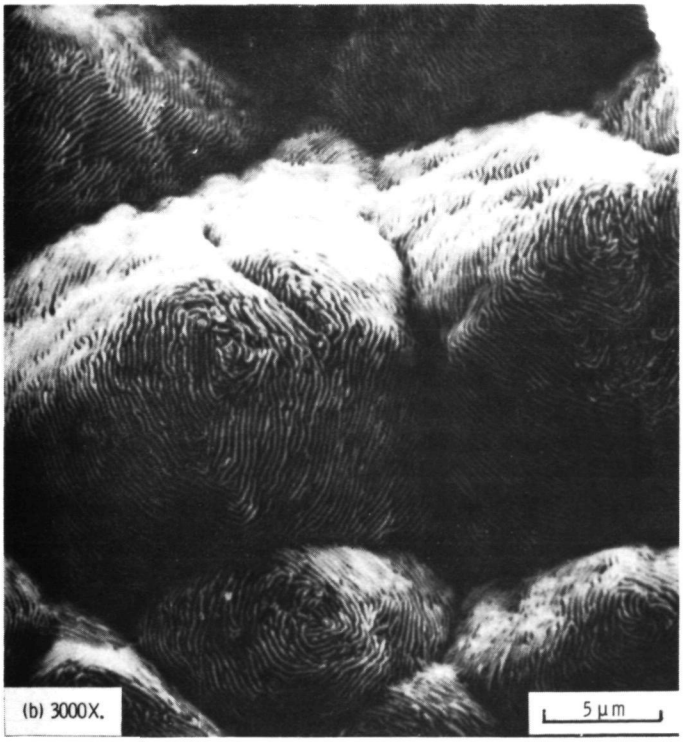

Figure 10. - SEM photographs showing typical ion beam-etched natural texture at three magnifications (25^0 tilt).

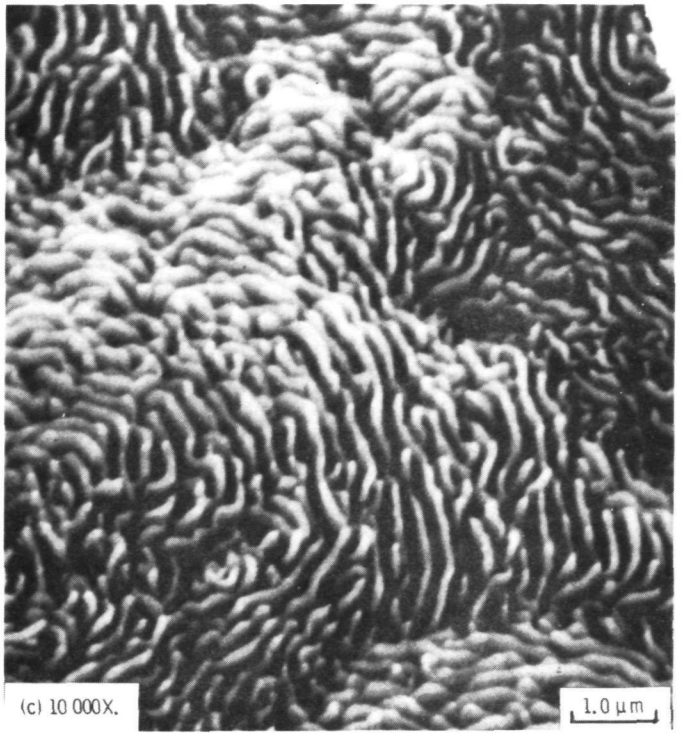

Figure 10. - Concluded.

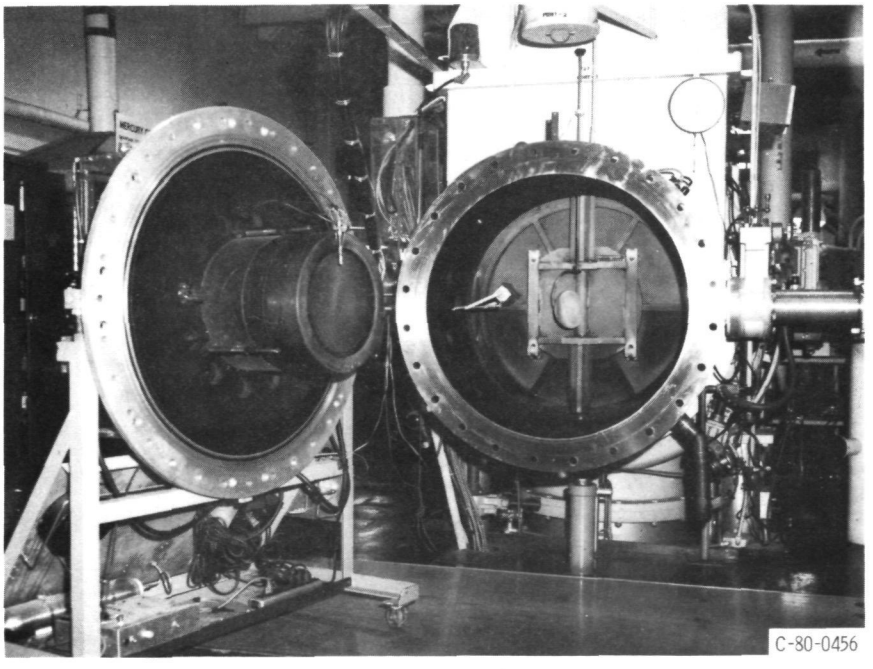

Figure 11. - 30-cm diameter argon ion source mounted in facility used for ion beam etching of square hole pattern.

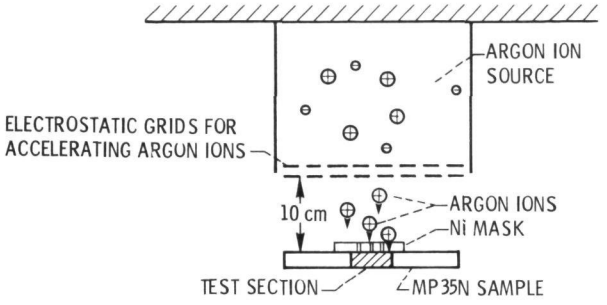

Figure 12. - Schematic arrangement of ion source and target specimen for ion beam sputter-etching of square hole pattern. Power supply arrangement given in reference 10.

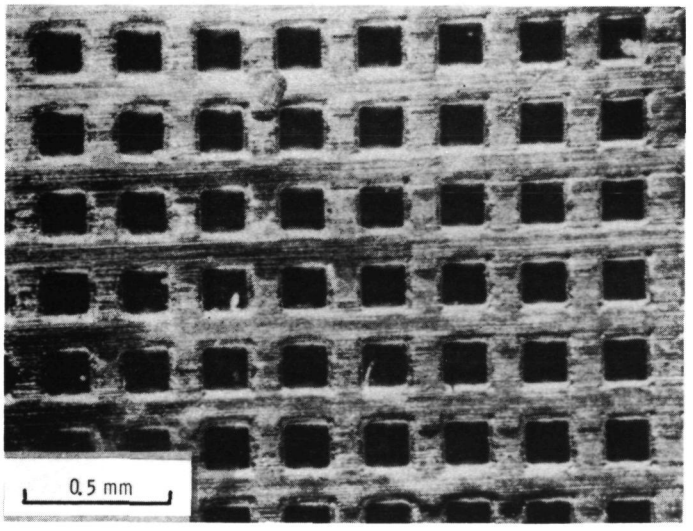

Figure 13. - Representative square hole pattern ion beam etched on MP35N surface (optical microscope, 40X). Edges of holes parallel to direction of rolling and longitudinal axis of fatigue specimen.

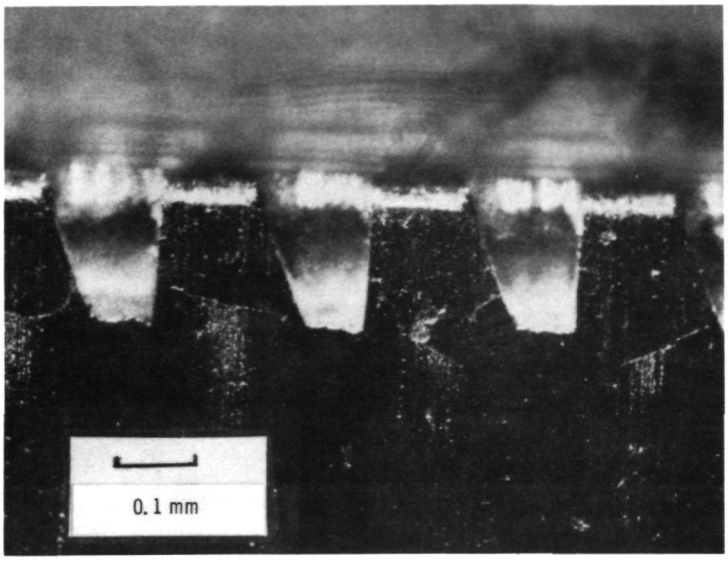

Figure 14. - Cross-section view showing tapered geometry of ion beam etched holes. (Optical microscope, 100X).

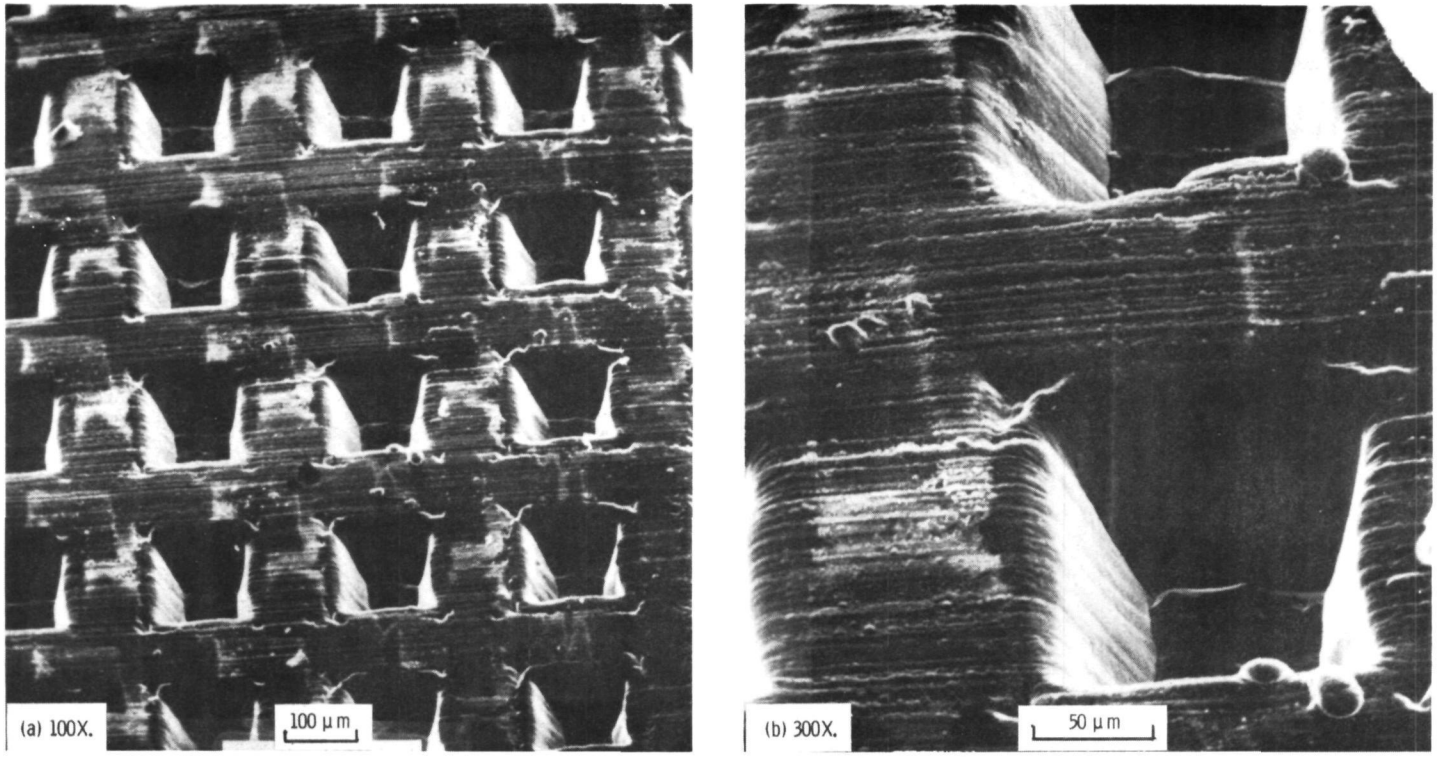

Figure 15. - SEM photographs of typical square hole structure at magnifications of 100X and 300X.

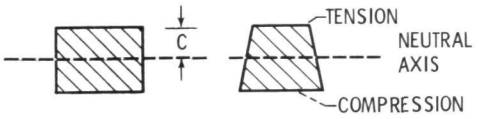

(a) UNSTRESSED. (b) STRESSED.

Figure 16. - Cross-section of fatigue specimen stressed and unstressed during pure bending.

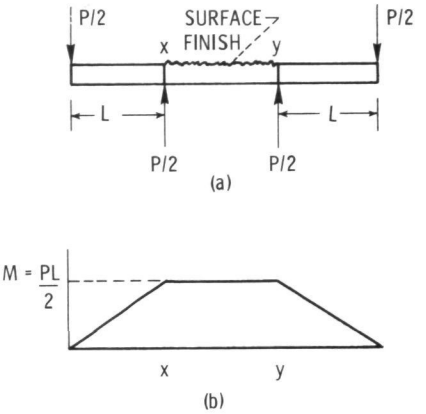

Figure 17. - (a) Free-body diagram showing distribution of load, P, in four-point bending mode; (b) Corresponding variation of bending moment, M, across specimen.

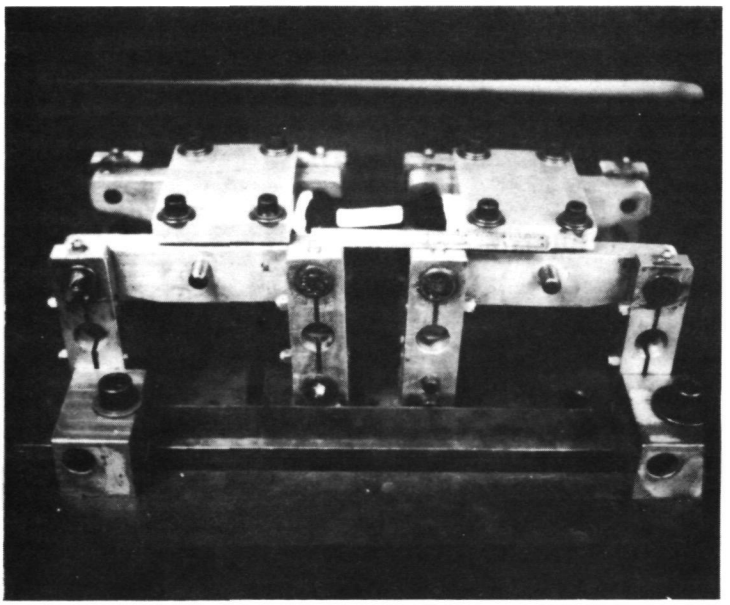

Figure 18. - Four-point bending fixture used in fatigue tests.

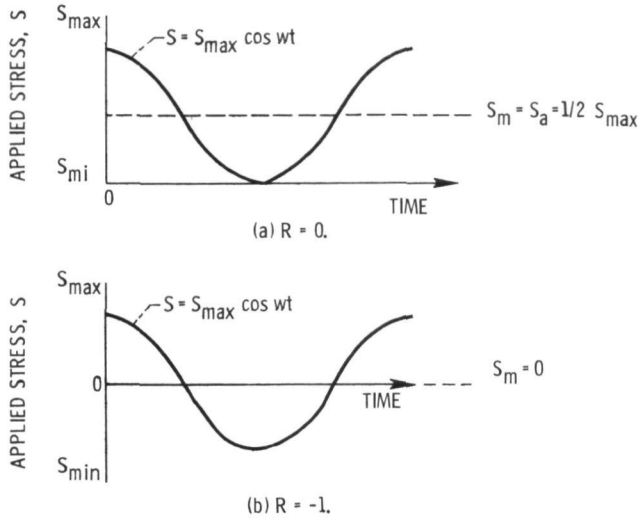

Figure 19. - Sinusoidal variation of applied stress for R = 0 and R = -1.

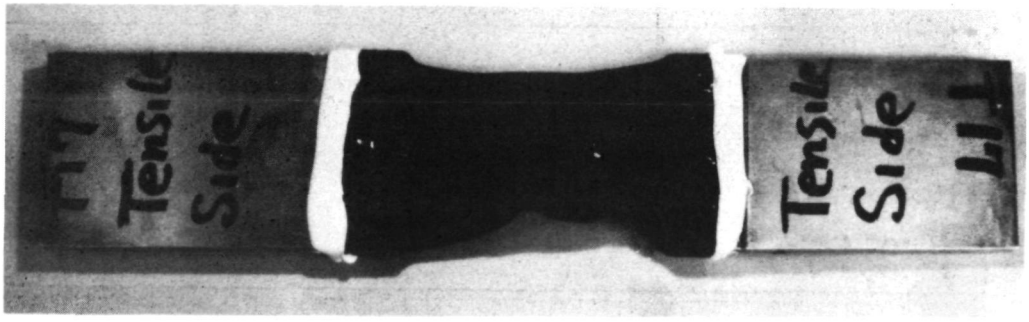

Figure 20. - Rubber tube containing physiological solution attached to fatigue specimen.

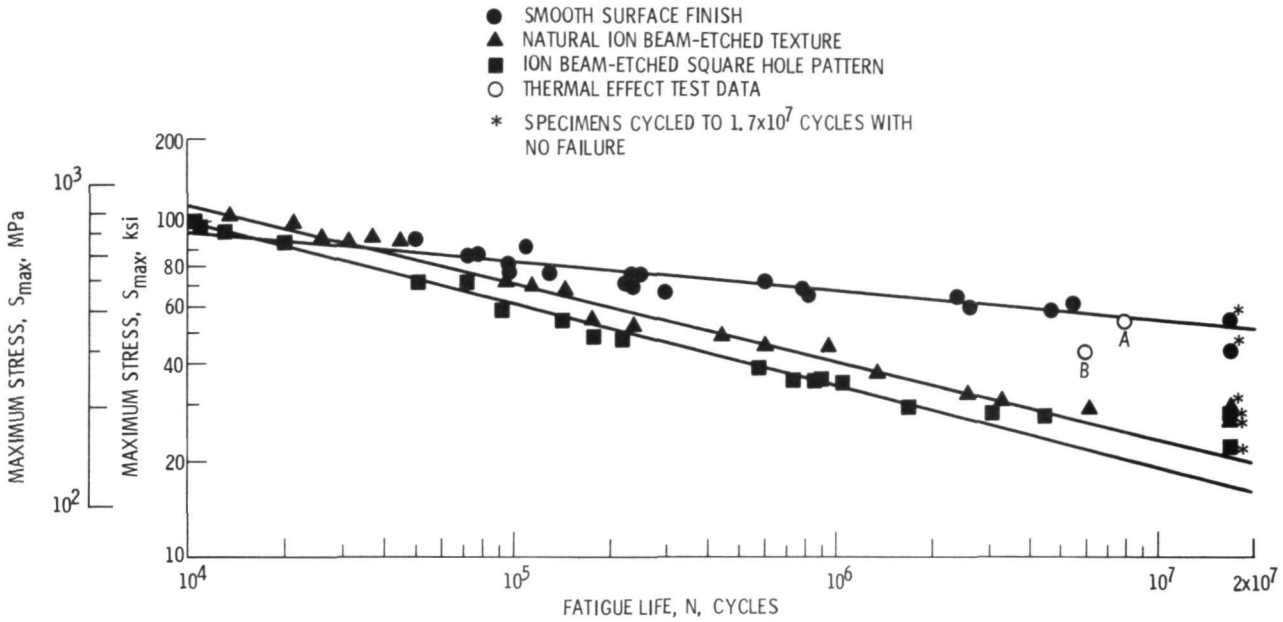

Figure 21. - S-N diagram (R = 0) of MP35N bending fatigue test results for each of three surface finishes. Straight lines fitted to test data by method of least squares. Points A and B are thermal effect test data for fatigue specimens with smooth surface finish heated for 2 hours to 500 and 660 C, respectively.) failure.

Figure 22. - Typical example of MP35N test specimen fatigue failure.

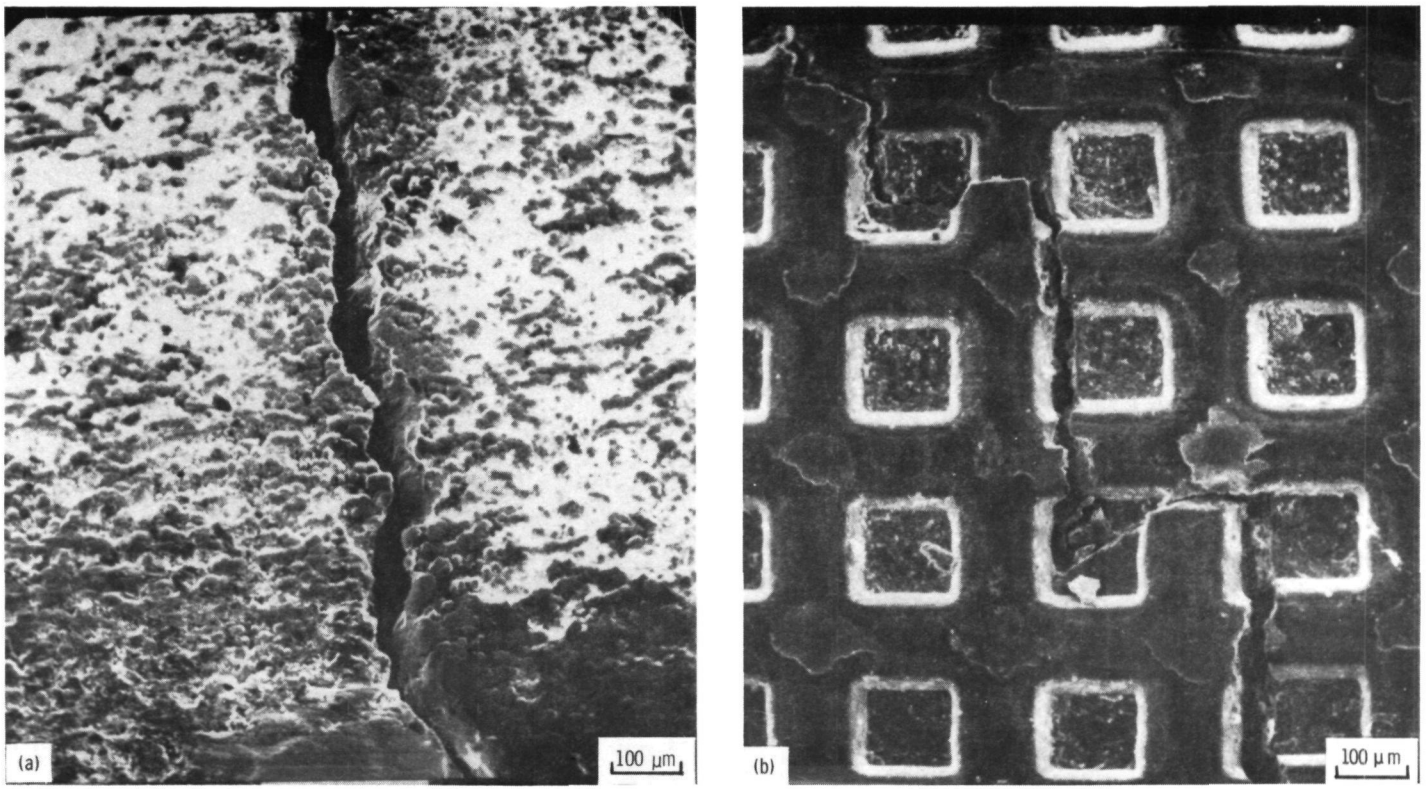

Figure 23. - SEM photographs of fatigue fractures of MP 35N specimens with (a) natural ion beam-etched texture and (b) pattern-etched surface structure.

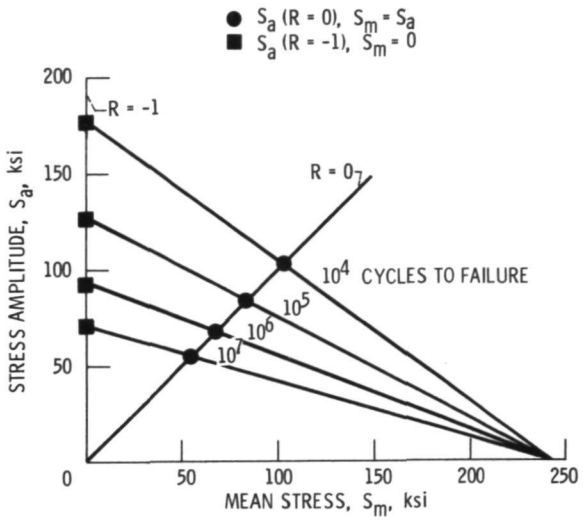

Figure 24. - Goodman's mean stress diagram for MP35N with smooth surface finish.

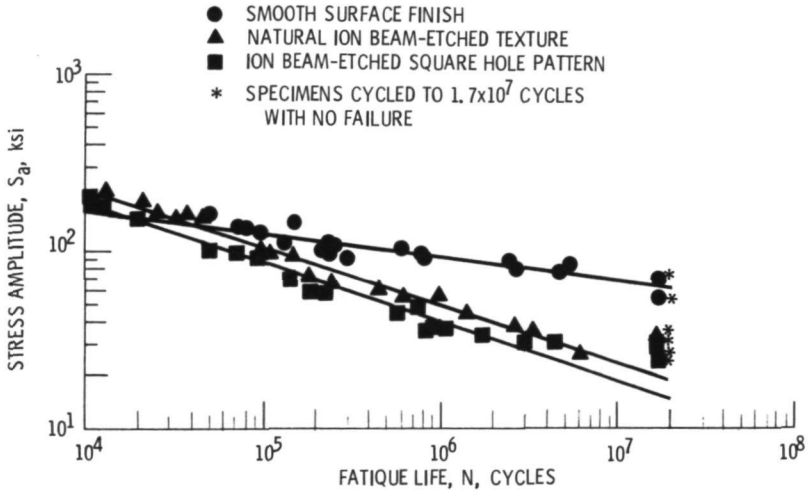

Figure 25. - S-N diagram of MP35N bending fatigue test results for each of the three surface finishes, R = -1.

1. Report No. NASA TM-81747	2. Government Accession No.	3. Recipient's Catalog No.
4. Title and Subtitle ION BEAM SPUTTER ETCHING OF ORTHOPEDIC IMPLANT ALLOY MP35N AND RESULTING EFFECTS ON FATIGUE PROPERTIES		5. Report Date March 1981 6. Performing Organization Code 506-55-32
7. Author(s) Edwin G. Wintucky and Mark Christopher, Lewis Research Center, and Eugene Bahnuik and Simon Wang, Case Western Reserve University, Cleveland, Ohio		8. Performing Organization Report No. E-782 10. Work Unit No.
9. Performing Organization Name and Address National Aeronautics and Space Administration Lewis Research Center Cleveland, Ohio 44135		11. Contract or Grant No. 13. Type of Report and Period Covered Technical Memorandum
12. Sponsoring Agency Name and Address National Aeronautics and Space Administration Washington, D.C. 20546		14. Sponsoring Agency Code

15. Supplementary Notes Prepared for the Fifteenth International Electric Propulsion Conference co-sponsored by the American Institute of Aeronautics and Astronautics, the Japan Society for Aeronautical and Space Sciences, and Deutsche Gesselschaft fur Luft- und Raumfahrt. Las Vegas, Nevada, April 21-23, 1981.

16. Abstract

The effects of two types of argon ion sputter etched surface structures on the tensile stress fatigue properties of orthopedic implant alloy MP35N were investigated. One surface structure was a natural texture resulting from direct bombardment by 1 keV argon ions. The other structure was a pattern of square holes milled into the surface by a 1 keV argon ion beam through a Ni screen mask. The etched surfaces were subjected to tensile stress only in fatigue tests designed to simulate the cyclic load conditions experienced by the stems of artificial hip joint implants. Both types of sputter etched surface structures were found to reduce the fatigue strength below that of smooth surface MP35N.

17. Key Words (Suggested by Author(s))	18. Distribution Statement
Ion beam sputter etching Orthopedic alloy MP35N Fatigue properties	Unclassified - unlimited STAR Category 26

19. Security Classif. (of this report)	20. Security Classif. (of this page)	21. No. of Pages	22. Price*
Unclassified	Unclassified		

* For sale by the National Technical Information Service, Springfield, Virginia 22161

National Aeronautics and
Space Administration

Washington, D.C.
20546

Official Business
Penalty for Private Use, $300

SPECIAL FOURTH CLASS MAIL
BOOK

Postage and Fees Paid
National Aeronautics and
Space Administration
NASA-451

U.S. MAIL

NASA

POSTMASTER: If Undeliverable (Section 158
Postal Manual) Do Not Return